metals

MDPI

Article

Examination of Behavior from Selected Foundry Sands with Alkali Silicate-Based Inorganic Binders

Iveta Vasková [1], László Varga [2], Ingo Prass [3], Viktoria Dargai [2], Martin Conev [4], Martina Hrubovčáková [1], Marianna Bartošová [1], Branislav Buľko [1,*] and Peter Demeter [1]

1 Faculty of Materials, Metallurgy and Recycling, Institute of Metallurgy, Technical University of Košice, 042 00 Košice, Slovakia; iveta.vaskova@tuke.sk (I.V.); martina.hrubovcakova@tuke.sk (M.H.); marianna.bartosova@tuke.sk (M.B.); peter.demeter@tuke.sk (P.D.)
2 Faculty of Materials Science and Engineering, Institute of Foundry, University of Miskolc, 3515 Miskolc, Hungary; laszlo.varga@uni-miskolc.hu (L.V.); dviki72@gmail.com (V.D.)
3 Nemak Linz, Zeppelinstrasse 24, 4030 Linz Austria; ingo.prass@nemak.com
4 Nemak Slovakia s.r.o., Ladomerská Vieska 394, 965 01 Žiar nad Hronom, Slovakia; martin.conev@nemak.com
* Correspondence: branislav.bulko@tuke.sk; Tel.: +421-55-602-3151

Received: 7 January 2020; Accepted: 5 February 2020; Published: 10 February 2020



Abstract: The automotive industry is one of the most important customers for the foundry industry. In particular, casting of engine parts for combustion engines is one of the most demanding areas of casting technology. New generation of engine blocks and cylinder heads are getting geometrically more complicated in order to maintain or even increase performance. With the increased complexity, the strain for the casting molds is growing and the widely used technology of core making with standard silica sands is, for several applications, no longer reaching the demanded results. Furthermore, in last decade, there has been an effort in using inorganic binders in core making process, which brings along some additional technological challenges. In order to cope with these challenges, in this paper, silica and non-silica sands with round and angular grains as well as with fine and coarse grains are examined using an inorganic binder for strength, permeability, and thermal stability. The results shall provide useful information about the possibilities of application and combining different types of foundry sands, both silica and non-silica. With their impact on the selected sand core properties, they can help in solving problems in the core making process as well as reaching a high quality of the final product-casting.

Keywords: foundry sand; grain shape; grain size; inorganic binder; sand cores; strength; permeability; thermal stability

1. Introduction

The main component of each sand mold is the base molding material, foundry sand, which is usually up to 98% of the whole mass depending on the used technology. For the production of molds or cores, natural or synthetic grains can be used [1]. Foundry sand is, according to the authors of [2], defined as granular refractory material with grains of sizes in a range from 0.02 mm to 2 mm. The most important foundry sand used is silica sand. The main component is quartz, a crystalline form of SiO_2. Silica sand is available in good quality in central Europe, which forms the basis for wide use in the foundry industry. However, silica sand has some negative properties, which can result in problems when producing high-quality cast parts. Practical experience and molding data show that 40–70% of the casting defects arise from inadequate mold properties [3]. The main disadvantage of silica sand is the thermal expansion behavior as a result of a phase transition. Silica sand has three modification changes (at 573 °C, 870 °C, and 1470 °C), which are connected to the change of density

and length. At 573 °C, reversible change of a modification β ↔ α-SiO2 takes place, which is connected to the increase of volume by 2,4%. At 870 °C, volume expansion grows to 14.8% owing to further modification to a high temperature polymorph of quartz called α-tridymite. At very high temperatures (1470 °C), slow modification to α-cristobalite takes place. The second negative property is a low sintering temperature (1450–1550 °C), which can be even lower in the presence of impurities such as alkaline oxides. Another drawback that can be mentioned is low thermal conductivity. All these well-known negative properties often lead to the use of alternative base materials—special non-silica sands. The authors of [4] presented that sand grain morphology has a significant influence on the bending strength of cores produced by cold box process. The author of [5] examined the technological properties of cores produced by water glass ester process with silica and non-silica foundry sands. In the selection of the base-molding material, it is essential to consider a number of factors, such as the type of alloy, size of casting, and casting process technology [2,6].

This paper will deal with the examination of different foundry sands with an alkali silicate-based binder cured by heat application for the production of cores for automotive parts from aluminum alloys. Despite the knowledge accumulated in the use of sodium silicate molding technology, it is not always possible to predict how a new commercial binder system will behave with untested refractory sands. Most new generation inorganic binders come in two components, a liquid part (the binder) and powder additive. The two-component systems were successfully implemented in the large-scale production of aluminum engine heads and blocks. The additives in the powder component optimize the sand mixture flowability, hardening rate, core strengths, cores storage, and thermal stability, and prevent the casting surface from burning on [7,8]. The main aspect of this paper was the analysis of how properties of one basic coarse sand can be influenced and changed by the addition of a fine sand (AFS). Basic material was a commonly used foundry sand (A coarse) from a Slovak sand mine characterized by an AFS grain fineness number (AFS GFN) of 40 (MK 0.39 mm) and a rounded grain morphology. AFS grain fineness number is a measure of average grain size and represents the number of openings per inch of a sieve that would pass the average size calculated from the sieve analysis. MK represents calculated average grain size from sieve analysis [9]. In order to cover a wide variety of sand properties, four different fine sands with a comparable grain size distribution, but with different properties such as grain shape, average grain size, and chemical and mineralogical composition were selected.

Sand type A fine is eolic silica sand with a rounded grain shape from the same source as the basic material [10]. Sand B is silica sand with angular grains, and thus is not commonly used in aluminum casting technology from a locality in Czech Republic [11]. Sand C is special foundry sand produced by fusing and super-cooling bauxite in an electric arc furnace. Sand C is characterized with spherical shaped grains [12,13]. Sand D is artificial sand made of mullite crystals by firing spherical granules. Both synthetic sands are produced in Asia [13,14]. Table 1 presents an overview, and the pictures in Figure 1 show the grain shapes and surfaces of the chosen sands for examination.

Table 1. List of tested sands. GFN, grain fineness number.

Type	Origin	Chemical Composition	Main Impurities	Grain Shape	AFS GFN
A Coarse	Slovakia	Silica (97.6% SiO_2)	Al_2O_3 (1.3%), K_2O + Na_2O (0.9%)	rounded	40
A Fine	Slovakia	Silica (96.3% SiO_2)	Al_2O_3 (2%), K_2O + Na_2O (1.4%)	rounded	70
B	Czech	Silica (99.2% SiO_2)	K_2O + Na_2O (0.1%)	angular	65
C	Asia	Synthetic bauxite (>85% Al_2O_3, <10% SiO_2)	Fe_2O_3 (<3%)	spherical	65
D	Asia	Synthetic mullite (61% Al_2O_3, 36% SiO_2)	not specified	spherical	65

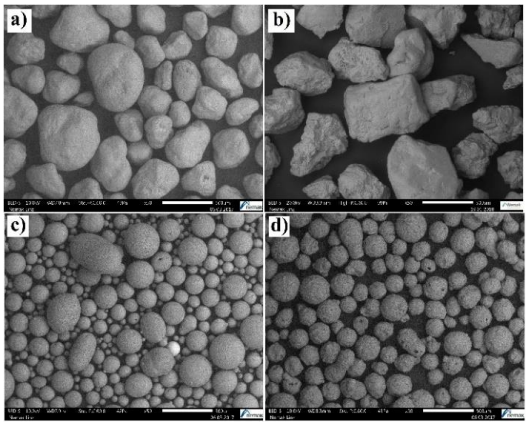


Figure 1. SEM pictures (×50) of tested sand types: (**a**) sand A; (**b**) sand B; (**c**) sand C; and (**d**) sand D.

2. Work Methodology and Materials

2.1. Sieve Analysis

According to the author´s previous research work [9], combining fine and coarse silica sands in specific ratios results in an increase of compaction and strength. Within this work, a wider choice of sands and properties were examined. Sands were combined in 10 wt.% addition steps and fine sands were added to coarse. Sieve analysis of sands and their combinations was condcuted as well as measurement of loose sand permeability.

2.2. Permeability Measurement

The permeability was measured using a Simpson digital absolute permmeter (Simpson Technologies GMBH, Euskirchen, Germany) with base permeability accessory provided by Simpson Technology. The permmeter determines how easily air can pass through the porous material. Permeability is determined by measuring the time required for air at AFS standard volume and pressure to pass through the sand specimen. In contrast to the common procedure, the authors decided not to measure the permeability of cylindrical core specimens, but of compacted loose sand [15]. With this procedure influence, factors of core production of the cylindrical core samples (blow pressure, sand level in core blowing machine, age of sand mixture, and so on) can be excluded, resulting in good reproducible measurement results.

The base permeability accessory consists of a calibrated metal tube, screen, and compacting weight (Figure 2) [16]. The tube is filled and the compacting weight is placed on top of the sand. This assembly is tapped until the compacting weight finishes settling and the sand has achieved its maximum density. Then, the weight and top portion of the tube are removed and the excess sand is struck off. The gas permeability number is non-dimensional [17].



Figure 2. Simpson digital permmeter.

2.3. Bending Strength

The sand mixtures for bending strength and hot distortion measurement were produced with a two-component inorganic binder system. For all mixtures, the amount of liquid binder was 2.0 wt.% and the amount of powder additive was 0.9 wt.%. Preparation of the mixture was done accordingly:

- Dry mixing of sands for 60 s;
- Dry mixing of sands with powder additive for 60 s;
- Mixing with liquid part of binder for 60 s;
- Storage of prepared mixture in closeable container in order to prevent drying during samples production.

Samples for measurement of bending strength (170 mm × 22.5 mm × 22.5 mm) were produced using the Benetlab laboratory core blower (Benetlab s.r.l., Passirano, Italy) (Figure 3) according to blowing and curing parameters published in the work of [9].



Figure 3. Benetlab laboratory core blower.

The measurement of bending strength is done as a basic characteristic property for molding materials; it depends on the binder system used and its dosage, as well as on the base material used and its properties (chemical, mineralogical, grain shape, grain size). In this examination, a universal strength machine LRu-2e Multiserw Morek (MULTISERW-Morek, Brzeźnica, Poland) (Figure 4) was used. Measurement was done after 30 s (immediate strength), after 1 h (cold, final strength), and after 24 h (samples were stored in desiccator).



Figure 4. Universal strength machine Lru-2e.

2.4. Hot Distortion Test

The hot distortion test was originally used to control the quality of shell molding materials. In this test, the behaviour of different molding materials from the point of view of time-dependent deformation and fracturing can be examined. The principle of the hot distortion test is shown in

Figure 5. The specimen is fixed on one end and heated from the bottom at the temperature of 1000 °C. From the obtained curve (height of deformation in time), thermoplastic or brittle behavior can be evaluated [1].

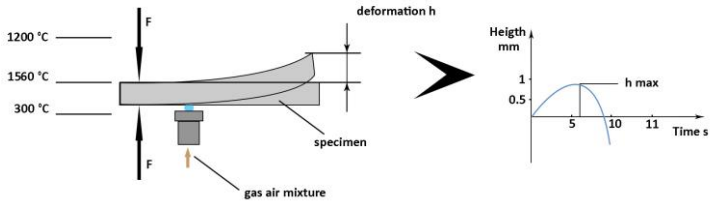


Figure 5. Scheme and principle of the HD (High Distortion) test [1].

Samples for the measurement of hot distortion test (114.3 mm × 25.4 mm × 6.35 mm) were produced at university of Miskolc using a Simpson Gerosa core laboratory blowing machine (Simpson Technologies GMBH, Euskirchen, Germany) with the following core blowing and curing parameters:

- Core box temperature 150 °C with 30 s curing time.

For the hot distortion analysis, the BCIRA measurement device (Simpson Technologies GMBH, Euskirchen, Germany) of the company Simpson Gerosa was used (Figure 6) [17].



Figure 6. BCIRA hot distortion tester.

3. Results

3.1. Sieve Analysis

The sieve analysis, as a one of the basic tests of every foundry sand, was done for each examined sand and their combinations. From the sieve analysis, basic information about sand properties can be obtained. Figures 7–10 present the grain size distribution curves for each tested sand combination and Tables 2–5 present the basic properties of tested sand combinations obtained or calculated from the sieve analysis. The authors have chosen the fines content as the measurement value and average grain size MK, theoretical surface S_{th}, and AFS GFN as the calculated characteristics.

Based on the sieve analysis of sands A coarse and A fine (Figure 7 and Table 2), it can be seen that more than 80% of sand grains of pure sands are distributed over two sieves, which is very desirable from the point of view of permeability and strength, as combining sands results in distribution over three to four sieves in the case of a 60:40 and 50:50 combination ratio, which can result in worse permeability as well as lower strength. Additionally, sand A fine has a high amount of fines content, and is thus the finest sand in this examination with the highest AFS value and the smallest MK value.

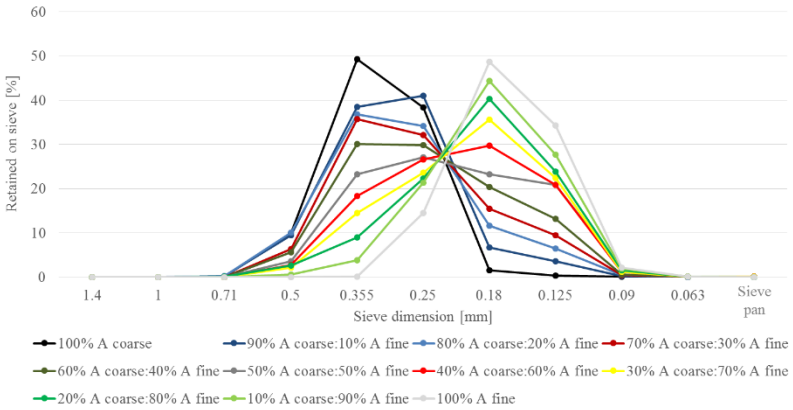


Figure 7. Grain size distribution curves for sands A coarse and A fine.

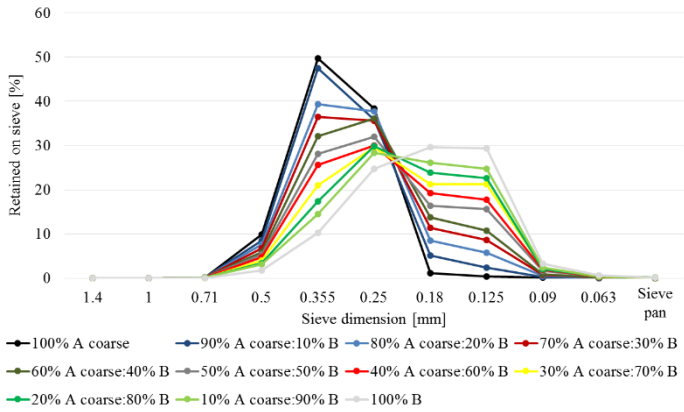


Figure 8. Grain size distribution curves for sands A coarse and B.

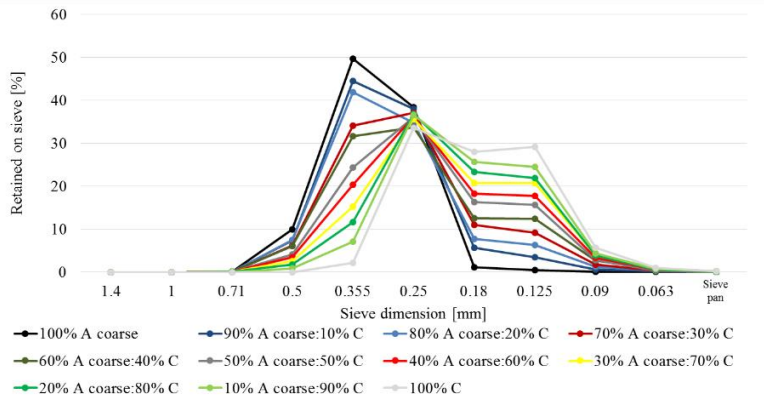


Figure 9. Grain size distribution curves for sands A coarse and C.

The grain size distribution of sand B (Figure 8 and Table 3) shows a smooth distribution of grains over three to four sieves, which, combined with the angular shape and high amount of fine particles, is the worst scenario for foundry sand, which can result in low strength, permeability, and flowability of the mixture.

Figure 9 and Table 4 show the results from the sieve analysis for sands A coarse and C. Sand C has grain size distribution over three sieves and a very high amount on the sieve with a mesh size of 0.09 mm. This, in the case of artificial sand, is not considered as a problem from the point of view of obtained strength. Figure 10 and Table 5 present the sieve analysis results for the combination of A

coarse and D. Sand D is also distributed over three sieves, but on the other hand, its fines content is around 1%, which, for foundry sands, is suitable.

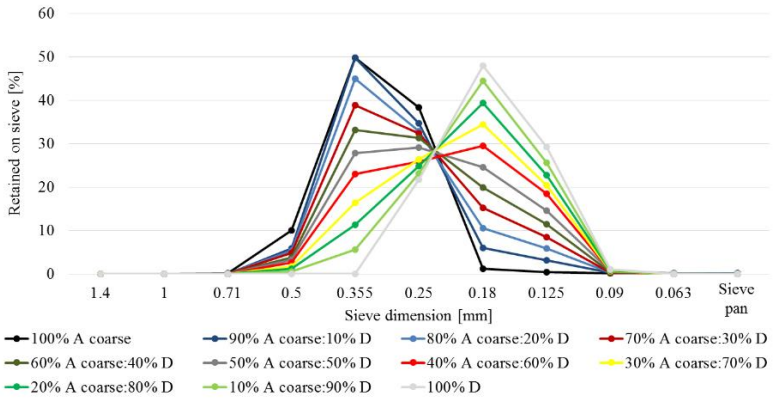


Figure 10. Grain size distribution curves for sands A coarse and D.

Table 2. Basic properties of sands A coarse and A fine.

A Coarse [%]	A Fine [%]	S_{th} [$cm^2.g^{-1}$]	AFS GFN	MK_{calc} [mm]	Fines Content < 0.125 mm [%]
100	0	61.45	42.8	0.387	0.286
90	10	67.70	46.1	0.364	0.281
80	20	71.91	46.5	0.354	0.527
70	30	77.72	48.3	0.332	0.770
60	40	83.24	51.1	0.314	0.729
50	50	93.52	56.6	0.283	1.850
40	60	96.61	60.3	0.270	1.507
30	70	100.57	63.3	0.256	1.507
20	80	104.01	65.4	0.244	1.709
10	90	110.72	68.5	0.221	2.118
0	100	118.24	72.6	0.201	2.368

Table 3. Basic properties of sands A coarse and B.

A Coarse [%]	Sand B [%]	S_{th} [$cm^2.g^{-1}$]	AFS GFN	MK_{calc} [mm]	Fines Content < 0.125 mm [%]
100	0	61.45	42.8	0.387	0.286
90	10	65.29	43.7	0.374	0.446
80	20	71.56	46.4	0.353	0.792
70	30	75.67	47.7	0.339	0.999
60	40	79.33	49.4	0.326	1.134
50	50	87.00	51.6	0.308	2.273
40	60	90.29	53.5	0.297	2.442
30	70	95.36	56.4	0.281	2.831
20	80	98.23	58.8	0.271	2.691
10	90	101.57	61.4	0.261	3.051
0	100	109.13	66.3	0.239	4.149

Table 4. Basic properties of sands A coarse and C.

A Coarse [%]	Sand C [%]	S_{th} [$cm^2.g^{-1}$]	AFS GFN	MK_{calc} [mm]	Fines Content < 0.125 mm [%]
100	0	61.45	42.8	0.387	0.286
90	10	68.04	45.0	0.363	0.883
80	20	72.44	45.8	0.353	1.567
70	30	78.82	48.5	0.331	2.271
60	40	84.33	49.7	0.319	3.496
50	50	89.32	52.7	0.297	3.270
40	60	93.91	54.6	0.284	4.012
30	70	99.76	57.4	0.267	4.904
20	80	101.67	59.2	0.256	4.496
10	90	107.14	62.4	0.240	5.337
0	100	115.09	67.6	0.220	6.889

Table 5. Basic properties of sands A coarse and D.

A Coarse [%]	Sand D [%]	S_{th} [$cm^2.g^{-1}$]	AFS GFN	MK_{calc} [mm]	Fines Content < 0.125 mm [%]
100	0	61.45	42.8	0.387	0.286
90	10	66.61	43.9	0.367	0.415
80	20	71.11	45.5	0.351	0.375
70	30	75.80	47.8	0.334	0.372
60	40	81.20	50.4	0.315	0.448
50	50	86.83	53.5	0.298	0.725
40	60	92.15	58.2	0.280	0.689
30	70	96.92	61.5	0.262	0.745
20	80	101.49	64.2	0.247	0.758
10	90	106.83	66.9	0.229	0.907
0	100	112.29	69.4	0.211	1.055

3.2. Permeability of Loose Sand

The permeability of foundry sand and thus core or mold significantly influences the quality of the casting. During metal pouring and cooling, the formation of gases from different sources occurs. Sand molds and cores must ensure an optimal passage of these gases before melt solidifies, otherwise gas bubbles can be trapped in the casting, causing, for example, a decrease of mechanical properties [18].

From the results of the permeability measurement (Figure 11), it can be stated that even a small addition of fine sand to coarse sand decreases the loose sand permeability by 25–40%. The permeability is steadily almost exponentially decreasing with the addition of more fine sand reaching its minimum in the pure fine sands. The biggest drop in permeability was observed when mixing A coarse with A fine. The explanation is that here, the effect of A fine as finest sand with the smallest MK value and highest fines content resulting in the lowest permeability of the chosen fine sand. One of the added fine sands shows a significant deviant behavior. When adding up to 20% of C, the permeability stays on the same high level for pure A coarse. Up to a 50:50 mix of A coarse with C, the permeability stays on a significant high level. This is noticeable especially in comparison with sand D. Both C and D are synthetic sands with an almost perfect round grain shape. C has significantly higher fines content than D and the permeability of pure C is slightly lower than that of pure D.

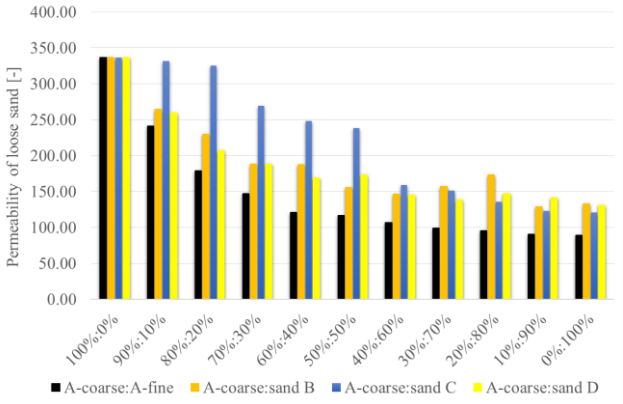


Figure 11. Results of the measurement of loose sand permeability.

3.3. Bending Strength

Mixing coarse and fine A sands results in the strength behavior presented by Figure 12. The minimum strength is reached at 100% A fine sand and local minimums at 100% A coarse and a 50:50 mix. Maximum strength is reached at a 60:40 mix, but high strength is also reached at 70:30, 40:60, and 30:70 ratios. This was already explained by examining the grain size distribution in the work of [9].

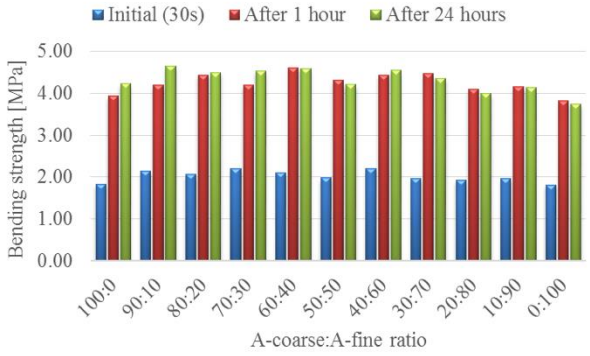


Figure 12. Strength behavior for sand combination A coarse and A fine.

The addition of sand B to coarse A sand had a negative effect on the strength level (Figure 13). This can be explained by the angular grain shape, and the grain size distribution over three to four sieves and a high amount of dust, which confirmed the earlier prediction based on the sieve analysis.

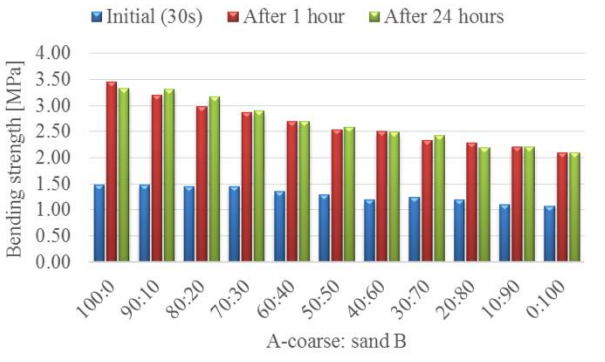


Figure 13. Strength behavior for sand combination A coarse and sand B.

In the case of mixing A coarse and C, almost linear dependence can be seen—the more C added, the higher the strengths measured (Figure 14). Adding 20% of C leads to an increase of immediate strength by 22.5%, and 30% addition of C also increases the final strength (after 1 h) by 18.75%. The final strength of 100% C is higher by 77% compared with 100% A coarse.

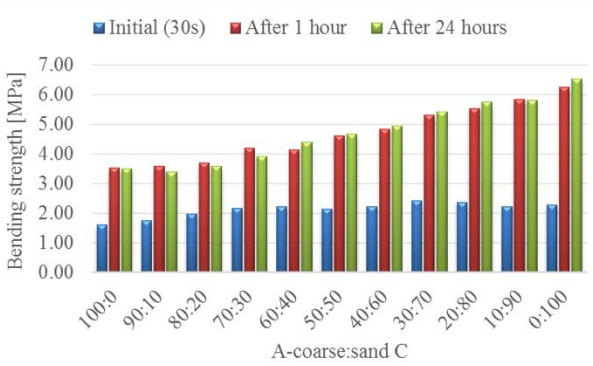


Figure 14. Strength behavior for sand combination A coarse and sand C.

The high bending strength of bauxite based sand was already observed and described by Iden, Tilch, and Wojtas for an organic cold box binder [4]. The high bending strength can be explained by two criteria; on the one hand, the perfect round shape granulometry and, on the other hand, the surface structure. The round grain shape is the basis for a good compaction and the possibility of a maximum number of surface contacts inbetween the grains. Furthermore, several of the C type sand grains have a well-defined surface structure with evenly distributed micro openings, which allow the binder to penetrate the surface and anchor the binder bridge. Using SEM technology, cohesive type of binder bridge destruction behavior, typical for inorganic binders, was observed in the analysed sand samples (Figure 15) [19].

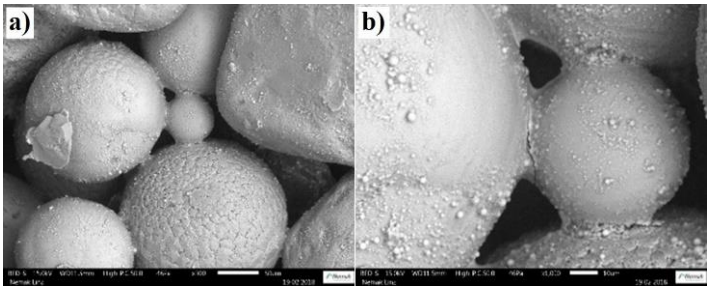


Figure 15. SEM pictures of bonded sand C, (**a**) ×500 and (**b**) ×1000, with a visible cohesive broken binder bridge.

In contrast to sand C, addition of D into A coarse resulted in a linear dependence, but compared with the influence of C, it has the reverse effect—the more D added, the lower the strengths (Figure 16). This is because of the large surface of D and the high water suction capacity of grains [1,12,14]; therefore, when D is introduced to the silica sand or is used as the base material, the binder amount must be increased in order to preserve strength level needed, especially when using fine grained D AFS 65.

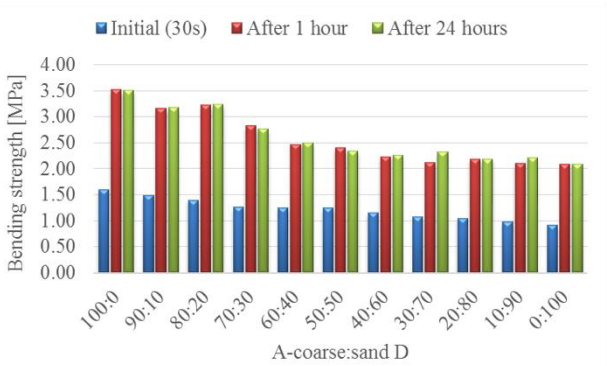


Figure 16. Strength behavior for sand combination A coarse and sand D.

3.4. Hot Distortion Test

The hot distortion test was performed only for test bars made of pure sands and their 50:50 combinations. In Figure 17, there are curves obtained by the measurement of hot distortion for pure sands. From the results, a significant difference between silica and non-silica sands can be seen. D sand has almost no deformation (0.04 mm), meanwhile fine A sand has almost 20 times higher deformation (0.76 mm). This can be explained by the completely different chemical and mineralogical nature of artificial sands, resulting in lower thermal expansion. The distinct thermoplastic behavior of the cores from the A sand type is remarkable. In contrast to the other sands, which reach the maximum measurable deformation after 30 or 40 s, A fine reaches the maximum measureable deformation after 60 s, and A coarse after 82 s (Figure 17). A feasible explanation for this behavior was not found within this investigation.

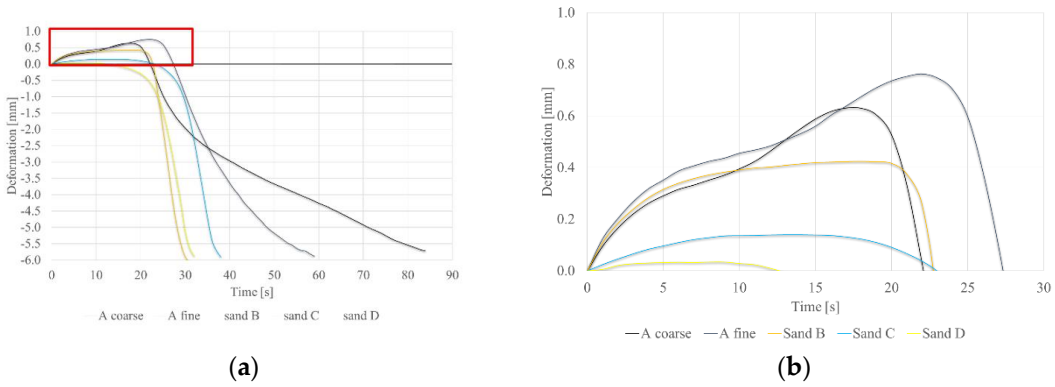
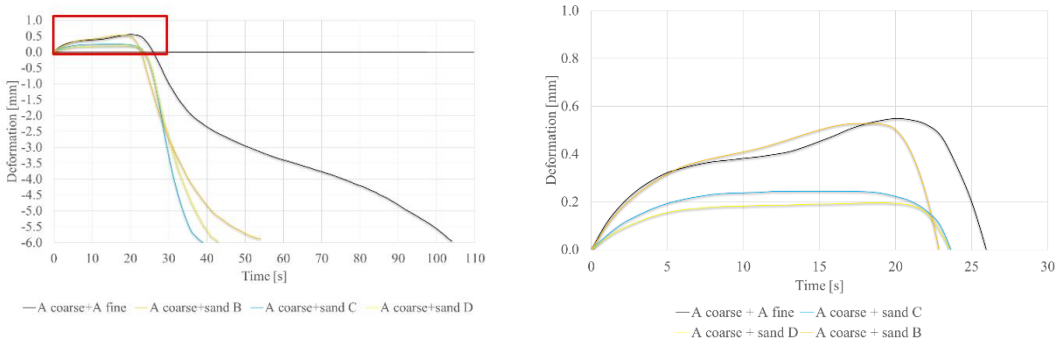


Figure 17. Hot-deformation curves of specimens made of tested sands: (**a**) general view, (**b**) detail.

The graph in the Figure 18 displays the results of the hot distortion test for combinations of sands in 50:50 ratios. As can be seen from the obtained curves, combining coarse sand A with artificial sands has a positive effect on the significant decrease of the deformation. Combining A coarse sand with fine silica sands also shows a slight decrease of the deformation and maximizes the thermoplastic behavior. The 50:50 mixture of sand A coarse and A fine reaches the maximum measureable deformation after 103 s. Figure 19 presents the comparison of deformations for measured mixtures.



(**a**) (**b**)

Figure 18. Hot deformation curves of specimens made of mixing sands in a 50:50 ratio: (**a**) general view, (**b**) detail.

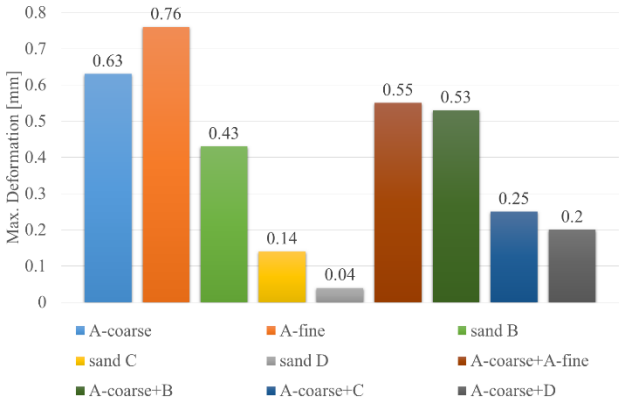


Figure 19. Maximal deformation of tested sands.

It is also important to state that, during the thermal load, test bars with alkali silicate-based binders do not break immediately after reaching the time of failure in contrast to test bars made of organic binders. This can be explained by the water glass basis of the binder systems. In contrast to organic binders, the binder bridge is not decomposing in the oxidation processes at thermal load, but when reaching its glass transition temperature, the binder becomes semi-fluid, which allows plastic deformation without breakage. Figure 20 shows deformed test samples after being exposed to thermal load.

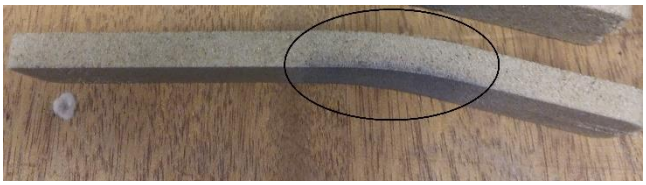


Figure 20. Deformed sample after hot distortion.

4. Summary and Conclusions

In this research work, different types of sand and their impact on basic properties of core and mold mixtures were investigated. Sands differed in granularity, grain shape, and mineralogical composition. Basic investigated properties were bending strength, permeability, and thermal stability. Using all sands as well as their combinations, mixtures with alkali silicate-based two-component binder system were prepared with the constant binder system amount in order to evaluate only the effect of the sand/sand combination on the basic observed properties. This research work provided a deeper insight

into the topic of the impact of sand properties on properties of the core or mold. Figure 21 presents the final comparison of properties obtained by the use of the tested base materials.

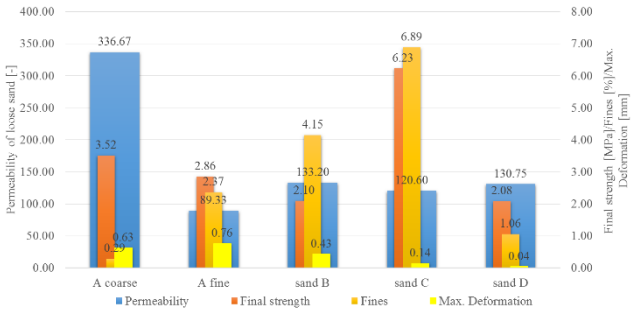


Figure 21. Final comparison of strength, permeability, fines content, and deformation of base materials.

The sieve analysis provided important information about average grain size, grain size distribution, and fines content of all tested sands. From this analysis, most favorable results were obtained for silica A coarse sand. Sand B had very wide grain size distribution and very high fines content. Artificial sand C had very high amount on the sieve with a mesh size 0.09 mm.

The thermal stability of silica sands is significantly lower than that of artificial sands. The best thermal stability was detected for sand D.

From the results of mixing A coarse with selected fine sands, the following observations can be summed up:

- Adding A fine resulted in the largest decrease of permeability, non-linear strength behavior, minor decrease of maximal deformation, and maximizing the thermoplastic bending behavior of A coarse;
- Addition of B caused a decrease of permeability and strength and a minor decrease of maximal deformation;
- Introducing C into A coarse had a minor effect on the drop of permeability up to 50% addition, bending strength increased significantly, and maximal deformation was reduced;
- Addition of D led to nearly the same decrease of permeability and bending strength as with B, but maximal deformation was the lowest with this sand.

The investigations show that the addition of a fine sand can lead to an improvement, but also to a decline of the physical properties of a base coarse sand, depending on the choice of the added fine sand. This information can help to avoid typical casting failures. The choice and amount of the added second sand is dependent on the casting challenge.

Author Contributions: I.V., author of main idea and technical revision; L.V., design of experimental part and technical revision; I.P., literature research, results interpretation, and technical revision; V.D., experimental work and results collection; M.C., experimental work and wrote the manuscript; M.H. and M.B. arranged the funding; B.B. and P.D. revised the original manuscript. All authors have read and agreed to the published version of the manuscript.

Funding: This research was funded by [VEGA MŠ SR a SAV] grant number [1/0868/17].

Conflicts of Interest: The authors declare no conflict of interest.

References

1. Polzin, H. *Inorganic Binders for Mould and Core Production in the Foundry*; Schiele & Schön GmbH: Berlin, Germany, 2014; pp. 146–149.
2. Jelínek, P. *Disperzní Soustavy Slévárenských Formovacích Směsí: Ostřiva*; Technical University of Ostrava: Ostrava, Czechia, 2000; pp. 10–15.

3. Krishnamoorthy, A. *Sand Control Practice in Ferrous Foundries*; Indian Institute of Foundrymen: Kolkata, India, 1991; pp. 43–46.
4. Iden, F.; Tilch, W.; Wojtas, H. Die Haftungsmechanismen von Cold-Box-Bindemitteln auf der Formstoffoberfläche. *Giesserei* **2011**, *98*, 24–36.
5. Polzin, H. Die Verfestigung von Alternativen Formgrundstoffen mit Anorganischen Bindersystemen. Available online: http://www.umweltstiftung.de/media/0405101027413fou.pdf (accessed on 16 December 2019).
6. Brown, R. *Foseco Ferrous Foundrymen Handbook*; Butterworth Heinneman: Oxford, UK, 2000; pp. 146–166.
7. Zaretskiy, L. Modified Silicate Binders New Developments and Applications. *Int. J. Met.* **2016**, *10*, 88–99. [CrossRef]
8. Banganayi, F.C.; Nyembwe, K.; Polzin, H. Effects of South African Silica Sand Properties on the Strength Development and Collapsibility of Single Component Sodium Silicate Binders. *Arch. Foundry Eng.* **2017**, *17*, 5–12. [CrossRef]
9. Conev, M.; Vasková, I.; Hrubovčáková, M.; Hajdúch, P. Impact of Silica Sand Granulometry on Bending Strength of Cores Produced by ASK Inotec Process. *Manuf. Technol.* **2016**, *16*, 327–334.
10. Ábelová, M.; Maglay, J. Viate piesky Záhorskej nížiny. *Enviromagazín* **2008**, *13*, 26–27. (In Czech)
11. Sklopísek Střeleč, A.S. Catalogue of Products. Available online: https://en.glassand.eu/our-sands/by-type/foundry-sands (accessed on 16 December 2019).
12. LKAB Minerals. Small Beads, Big Impact. Available online: https://www.lkabminerals.com/en/minsand-cheaper-than-zircon/ (accessed on 16 December 2019).
13. Recknagel, U.; Dahlmann, M. Special Sands-Base Materials for Modern Core and Mould Making. *Giess.-Rundsch.* **2009**, *56*, 6–17.
14. Wakita, K.; Matsubara, M. Characteristics and application of the round ceramic base sand CERABEADS. *Slevarenstvi* **2015**, *63*, 262–264. (In Czech)
15. Jelínek, P. Contribution of the Czechoslovak Foundry Industry to Chemization of Manufacture of Molds and Cores on the Base of Alcali Silicates. *Slevarenstvi* **1996**, *44*, 85–103.
16. Simpson Technologies Sandprüfgeräte. Available online: http://www.simpsongroup.com/media/deu/2015/07/Simpson-Analytics-Product-Catalog-US.pdf (accessed on 16 December 2019).
17. Simpson Gerosa BCIRA Hot-Distortion Tester. Available online: http://www.simpsongroup.com/model/42114 (accessed on 16 December 2019).
18. Ajibola, O.O.; Oloruntoba, D.T.; Adewuyi, B.O. Effects of Moulding Sand Permeability and Pouring Temperatures on Properties of Cast 6061 Aluminium Alloy. *Int. J. Met.* **2015**. [CrossRef]
19. Kamińska, J.; Angrecki, M.; Palma, A.; Jakubski, J.; Wildhirt, E. The effect of additive "B" on the properties of CO_2-hardened foundry sands with hydrated sodium silicate. *Arch. Metall. Mater.* **2017**, *62*, 1637–1641. [CrossRef]



© 2020 by the authors. Licensee MDPI, Basel, Switzerland. This article is an open access article distributed under the terms and conditions of the Creative Commons Attribution (CC BY) license (http://creativecommons.org/licenses/by/4.0/).